

Article

A Battery SOC Estimation Method Based on AFFRLS-EKF

Ming Li ^{1,*}, Yingjie Zhang ^{1,*}, Zuolei Hu ¹, Ying Zhang ² and Jing Zhang ³¹ College of Information Science and Engineering, Hunan University, Changsha 410000, China; huzuolei@hnu.edu.cn² School of Computer Science, Northwestern Polytechnical University, Xi'an 710000, China; ying_zhang@nwpu.edu.cn³ Institute of Industry Energy-Saving Control and Evaluation, Hunan University, Changsha 410000, China; zhangj@hnu.edu.cn

* Correspondence: minglee@hnu.edu.cn (M.L.); zhangyj@hnu.edu.cn (Y.Z.)

Abstract: The lithium-ion battery is the key power source of a hybrid vehicle. Accurate real-time state of charge (SOC) acquisition is the basis of the safe operation of vehicles. In actual conditions, the lithium-ion battery is a complex dynamic system, and it is tough to model it accurately, which leads to the estimation deviation of the battery SOC. Recursive least squares (RLS) algorithm with fixed forgetting factor is widely used in parameter identification, but it lacks sufficient robustness and accuracy when battery charge and discharge conditions change suddenly. In this paper, we proposed an adaptive forgetting factor regression least-squares—extended Kalman filter (AFFRLS-EKF) SOC estimation strategy by designing the forgetting factor of least squares algorithm to improve the accuracy of SOC estimation under the change of battery charge and discharge conditions. The simulation results show that the SOC estimation strategy of the AFFRLS-EKF based on accurate modeling can effectively improve the estimation accuracy of SOC.

Keywords: battery state of charge; parameter estimation; recursive least square; extended Kalman filtering

Citation: Li, M.; Zhang, Y.; Hu, Z.; Zhang, Y.; Zhang, J. A Battery SOC Estimation Method Based on AFFRLS-EKF. *Sensors* **2021**, *21*, 5698. <https://doi.org/10.3390/s21175698>

Academic Editor: Andrea Facchinetti

Received: 26 July 2021

Accepted: 20 August 2021

Published: 24 August 2021

Publisher's Note: MDPI stays neutral with regard to jurisdictional claims in published maps and institutional affiliations.



Copyright: © 2021 by the authors. Licensee MDPI, Basel, Switzerland. This article is an open access article distributed under the terms and conditions of the Creative Commons Attribution (CC BY) license (<http://creativecommons.org/licenses/by/4.0/>).

1. Introduction

The main purpose of the battery management system (BMS) is to ensure the safe operation of the batteries [1]. State evaluation of a battery, including state of charge, state of health, and state of life, is a critical task for a BMS. As the power source and energy storage equipment in the actual operation of electric vehicles, the battery will carry out continuous charging and discharging operations, and the battery state remains changing. It is very important to predict the battery status in advance to adjust the battery management system in time and ensure the safe operation of the battery. As a key power source for hybrid electric vehicles, accurate acquisition of SOC is very important to improve the dynamic performance of the battery and optimize the energy management strategy [2,3]. Model-based SOC estimation is an important research direction. However, battery SOC is affected by many factors such as actual working conditions, ambient temperature, battery aging, and self-discharge rate [4], accurate modeling is difficult, which leads to the difficult problem of high-precision SOC estimation.

There is much research literature on battery SOC estimation methods. Ampere-hour measurement method is one of the traditional SOC estimation algorithms. Due to the unknown initial value of SOC and the existence of an integral part, the estimation error will gradually accumulate with the increase of the battery running time, so the ampere-hour measurement method is usually combined with other estimation algorithms [5,6]. The open-circuit voltage method [7] and the internal resistance characteristic method [8] have a good performance, however, it requires the battery to stand for a period, which is not conducive to online calculation. The estimation accuracy of battery

SOC is also affected by actual battery working conditions. The extended Kalman filter (EKF) has been successfully applied for the estimation of SOC in HEV BMSs. The traditional Kalman filter (KF) is used for linear problems, while EKF linearizes the prediction by using partial derivatives and Taylor series expansion [9]. The influence of acquisition accuracy of voltage, current, and other signals on SOC estimation is discussed in the view of the hardware [10]. To reduce the initial error of the Coulomb counting method (CCM), the SOC can be calculated accurately by applying the battery efficiency to the open-circuit voltage (OCV) [11]. The application of machine learning (ML) in the BMS of LIB has long been adopted for efficient, reliable, accurate prediction of several important states of LIB such as state of charge, state of health, and remaining useful life [12]. Electromagnetic interference (EMI) of battery management systems (BMSs) will cause measurement errors of current and voltage signals, which will affect the performance of BSM [13,14–19]. For the situation that battery working conditions change rapidly, a recursive calculation method based on the Kalman filter is adopted [20–22]. The algorithm considers the battery as a dynamic system, and the filter performs state recursion according to the input (current, voltage, temperature, etc.) to obtain the estimated value of SOC. The method has a strong suppression effect on noise and is suitable for the condition of rapid current variation. However, the algorithm involves complex matrix inversion operation, and the calculation accuracy depends on the precise battery model. As the temperature changes and the battery ages, the internal and external characteristics of the battery will change. To improve the accuracy of the battery dynamic model, it is necessary to identify the battery parameters online [23]. The recursive least squares (RLS) algorithm is an easy algorithm to implement. However, with the increase of data, phenomena such as data saturation will occur, and it cannot be used for parameter identification well. Moreover, due to its fixed forgetting factor, the robustness of the system is poor when disturbed [24]. The least-square algorithm with a forgetting factor (FFRLS) adds a forgetting factor on the basis of RLS algorithm to solve the problem of data saturation [25,26]. Battery parameter identification based on RLS and SOC estimation algorithm based on EKF is widely used [27–30]. In Literature [27], the model parameter identification deviation caused by current and voltage measurement noise was compensated to improve the parameter identification accuracy to improve the SOC estimation accuracy. In literature [28], decoupled double estimators were used to estimate SOC and battery capacity, and different time scales were used to improve the accuracy and stability of the model. A SOC estimation algorithm combining variable factor RLS and CKF was proposed in the literature [29] to effectively improve the accuracy of estimation. Considering SOC constraints and estimation errors, the literature [30] introduced gain factors based on EKF algorithm, and the proposed algorithm has good effects in terms of accuracy, convergence speed, and robustness.

However, none of the above methods focuses on the SOC estimation under the condition of battery charging and discharging state changes. When the current charging and discharging state changes, the battery system is disturbed, resulting in inaccurate parameter estimation which affects the accuracy of the modeling of the equivalent circuit of the battery, thus affecting the accuracy of battery SOC estimation. In order to improve the estimation accuracy of battery SOC, a precise modeling method based on parameter identification was proposed under the condition of battery charging and discharging state changes. An adaptive forgetting factor regression least-squares algorithm (AFF-RLS) was designed to improve the model parameter identification accuracy, and then the battery SOC is estimated by the extended Kalman filter algorithm.

The main contributions of this paper are as follows:

1. The paper proposed an AFFRLS-EKF SOC estimation strategy based on parameter identification modeling aiming at the uncertainty of battery model parameters under the condition of abrupt change of battery charge and discharge.
2. The second-order Thevenin equivalent circuit model (2-order ECM) of the battery was established, and the SOC-OCV relationship was obtained. According to the

charging and discharging conditions, a segment-adaptive recursive least square algorithm was designed to identify the parameters to improve the model accuracy.

3. The proposed estimation strategy is applied to numerical simulation experiments, and RLS–EKF and AFFRLS–EKF are compared. The latter one has better performance in accuracy and robustness.

2. Equivalent Circuit Model

The battery is a complex electrochemical system. An accurate description of battery internal and external characteristics is one of the solutions to improve the accuracy of battery SOC estimation. In order to accurately describe the battery characteristics, the electrochemical model [31–33], equivalent circuit model [34–36], electrochemical impedance model [10], and other model-based methods were proposed to solve the SOC estimation problem. The more accurate the battery model is to simulate the electrochemical processes that occur during the battery operation, the more accurate the model will be. The equivalent circuit model has been widely used due to its better model accuracy and higher computational efficiency [37]. Combined with the model accuracy, calculation amount, and feasibility analysis, the equivalent circuit model second-order Thevenin model is adopted. The second-order RC model can simulate the electrochemical polarization and concentration polarization of the battery, which is one of the most common models of lithium batteries in the actual operation of vehicles. Compared with the first-order Thevenin model, it can more accurately describe the actual characteristics of the battery. Figure 1 shows a second-order Thevenin equivalent circuit model.

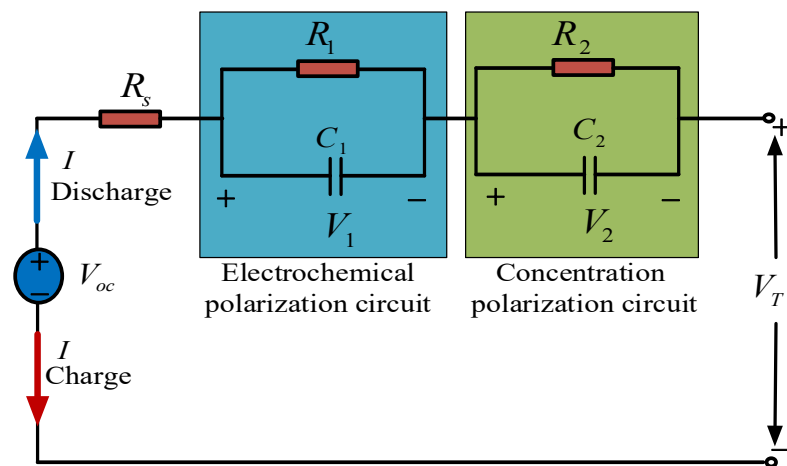


Figure 1. Thevenin equivalent circuit model.

As shown in Figure 1, when current I flows out of the positive electrode, the battery is in a state of discharge; otherwise, the battery is in a state of charge. V_{oc} is the battery's open-circuit voltage (OCV) which represents the nonlinear relation with the SOC of the battery. R_s is the ohmic resistance of the battery that represents the contact resistance between the electrode material and the electrolyte. The first RC network describes the polarization characteristics with R_1 , C_1 standing for polarization resistance and polarization capacitance, respectively. The second RC circuit illustrates the dynamic behavior of the battery along with concentration polarization, in which R_2 , C_2 represents the concentration polarization resistance and capacitance, respectively. V_T is the terminal voltage that can be measured directly.

We can fit the OCV–SOC relationship by using the OCV–SOC test, and the test results are shown in Table 1 [38].

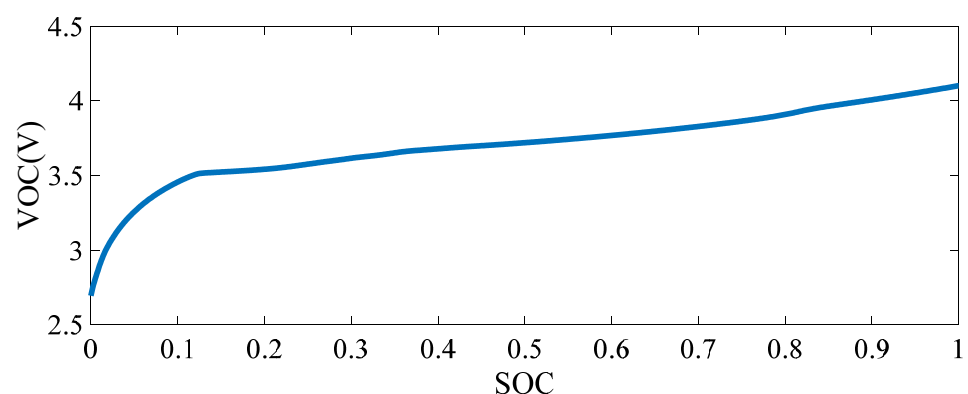
Table 1. Charging and discharging test data sheet.

SOC	VOC	SOC	VOC	SOC	VOC
0%	2.6936	35%	3.6504	70%	3.8270
5%	3.2567	40%	3.6776	75%	3.8627
10%	3.4552	45%	3.6982	80%	3.9073
15%	3.5220	50%	3.7184	85%	3.9628
20%	3.5408	55%	3.7414	90%	4.0056
25%	3.5750	60%	3.7670	95%	4.0510
30%	3.6144	65%	3.7954	100%	4.1000

Literature [39] studied the influence degree and computational complexity of temperature, data points, and aging degree on the lithium battery open-loop voltage model. The 11th-order polynomial fitting was selected, and the functional relationship between VOC and SOC was obtained as follows:

$$V_{oc}(SOC) = [0.3890SOC^{11} - 2.0452SOC^{10} + 4.6445SOC^9 - 5.9667SOC^8 + 4.7723SOC^7 - 2.4677SOC^6 + 0.8329SOC^5 - 0.1832SOC^4 + 0.0266SOC^3 - 0.0027SOC^2 + 0.0002SOC^1 + 0.0003SOC^0] \times 10^5 \quad (1)$$

The curve-fitted SOC–OCV correlation are shown in Figure 2.

**Figure 2.** Fitted Map of VOC–SOC.

According to Kirchhoff's voltage law, the circuit terminal voltage V_T is expressed as follows:

$$V_T = V_{oc} - R_s I - V_1 - V_2 \quad (2)$$

where V_1 represents the battery electrochemical polarization voltage, which is described as Equation (3). V_2 represents the battery concentration polarization voltage, which is described as Equation (4).

$$\frac{dV_1}{dt} = \left(\frac{1}{C_1}\right)I - \left(\frac{1}{R_1 C_1}\right)V_1 \quad (3)$$

$$\frac{dV_2}{dt} = \left(\frac{1}{C_2}\right)I - \left(\frac{1}{R_2 C_2}\right)V_2 \quad (4)$$

After modeling the Li-battery with Equations (2)–(4), the Li-battery model can be expressed in state-space equation form as follows:

$$\begin{cases} \frac{dSOC}{dt} \\ \frac{dV_1}{dt} \\ \frac{dV_2}{dt} \end{cases} = \begin{bmatrix} 0 & 0 & 0 \\ 0 & (1 + \frac{-1}{R_1 C_1}) & 0 \\ 0 & 0 & (1 + \frac{-1}{R_2 C_2}) \end{bmatrix} + \begin{bmatrix} \frac{-1}{C} \\ \frac{1}{C_1} \\ \frac{1}{C_2} \end{bmatrix} I \quad (5)$$

$$V_T = V_{oc} - R_s I - V_1 - V_2$$

where C represents the capacity of the Li-battery (Ah).

The battery model parameters are greatly affected by the system model and external disturbance. The RLS algorithm can accurately capture the real-time characteristics of the system by regularly correcting and updating the system parameters. Therefore, Equation (5) can be expressed in the s -domain as follows:

$$G(s) = \frac{V_T(s) - V_{oc}(s)}{I(s)} = - \left[R_s + \frac{R_1}{1 + R_1 C_1 s} + \frac{R_2}{1 + R_2 C_2 s} \right] \quad (6)$$

where s is for the frequency operator.

To ensure the consistency of system stability before and after transformation, the function was transformed from the s domain to the z domain by the bilinear transformation method.

$$s = \frac{2}{T} \frac{1 - z^{-1}}{1 + z^{-1}} \quad (7)$$

Substitute Equation (7) into Equation (6) and simplify to obtain the discrete transfer function of the system. Matlab solves the change from the s domain to the z domain to obtain the transfer function of Z domain, as shown in Equation (8).

$$G(z) = \frac{b_0 + b_1 z^{-1} + b_2 z^{-2}}{1 - a_1 z^{-1} - a_2 z^{-2}} \quad (8)$$

where $\{b_i | i = 0, 1, 2\}$, $\{a_j | j = 1, 2\}$ are the parameters to be identified. The relationship between model parameters and parameters to be identified is as follows:

$$\begin{cases} R_s = -\frac{b_0 - b_1 + b_2}{a_1 - a_2 + 1} \\ R_s + R_1 + R_2 = \frac{b_0 + b_1 + b_2}{a_1 + a_2 - 1} \\ R_1 C_1 R_2 C_2 = -\frac{T^2 (a_1 - a_2 + 1)}{4(a_1 + a_2 - 1)} \\ R_1 C_1 + R_2 C_2 = -\frac{T(a_2 + 1)}{a_1 + a_2 - 1} \\ R_1 C_1 (R_s + R_2) + R_2 C_2 (R_s + R_1) = -\frac{T(b_0 - b_2)}{a_1 + a_2 - 1} \end{cases} \quad (9)$$

T is the sample time.

Equation (8) can be rewritten in the difference equation form as:

$$E(k) = a_1 E(k-1) + a_2 E(k-2) + b_0 I(k) + b_1 I(k-1) + b_2 I(k-2) + \varepsilon(k) \quad (10)$$

where $E(k) = V_T(k) - V_{oc}(k)$.

Therefore, Equation (10) can be rewritten as follows in matrix form:

$$y(k) = \theta(k)^T \phi(k) + \varepsilon(k) \quad (11)$$

with,

$$\theta(k) = [a_1 \ a_2 \ b_0 \ b_1 \ b_2]^T \quad (12)$$

$$\phi(k) = [E(k-1) \ E(k-2) \ I(k) \ I(k-1) \ I(k-2)]^T \quad (13)$$

Equations (10)–(13) will be used in the RLS algorithm to estimate model parameters. Then the battery model parameters can be obtained by Equation (9) after $\theta(k)$ is estimated.

3. Adaptive Forgetting Factor Regression Least Squares

RLS can reduce the influence of application environment uncertainty on the system model and model parameters by periodic parameter correction and updating, to achieve the accurate acquisition of real-time characteristics of the system. In the RLS algorithm, the forgetting factor is a very important parameter, whose value will affect the convergence rate and sensitivity to noise of the algorithm [24]. Therefore, in this paper, the forgetting factor adaptive recursive least square method is used to estimate the parameters. When the battery charge and discharge conditions change suddenly, the adaptive forgetting factor is introduced to adjust the confidence ratio of the recursive model to the old data and the new data, to realize the accurate estimation of the model parameters. For the system model to be identified as shown in Equation (11), the recursion formula of the recursive least squares algorithm with forgetting factor is described as Equation (14) [40]:

$$\begin{cases} \hat{\theta}(k+1) = \hat{\theta}(k) + K(k+1) [y(k+1) - \varphi^T(k+1) \hat{\theta}(k)] \\ K(k+1) = \frac{P(k) \varphi(k+1)}{\lambda + \varphi^T(k+1) P(k) \varphi(k+1)} \\ P(k+1) = \frac{1}{\lambda} [I - K(k+1) \varphi^T(k+1)] P(k) \end{cases} \quad (14)$$

where, $k = 1, 2, 3, \dots$, $\hat{\theta}(k)$ and $\hat{\theta}(k+1)$ are the identifiable vectors of order k and order $k+1$ respectively, I is the identity matrix, λ is a constant forgetting factor in the range of 0 to 1, $K(k+1)$ is the correction gain vector, $P(k+1)$ and $P(k)$ are the covariance matrices of order k and order $k+1$, respectively.

When the battery charging and discharging conditions change suddenly, the system disturbance is large, and the instantaneous error of the parameters to be estimated is large, which affects the stability of the system. Therefore, the forgetting factor λ is designed to reduce the instantaneous error of the estimated parameters and increase the stability of the system. Since λ varies within the range of 0–1, the higher its value is, the stronger the anti-interference ability of the system will be. When the current change exceeds a certain value, it indicates that the current changes from charging state to discharging state or from discharging state to charging state. The rules for detecting current zero crossing are as follows:

$$\begin{cases} \delta = 0, & \frac{1}{2} |I(k) - I(k-1)| > \min(|I(k)|, |I(k-1)|) \\ \delta = 1, & \frac{1}{2} |I(k) - I(k-1)| \leq \min(|I(k)|, |I(k-1)|) \end{cases} \quad (15)$$

where, δ indicates whether the charging state of the battery has changed, $\delta=1$ represents the battery changing from charging state to discharging state or the battery changing from discharging state to charging state, $\delta=0$ indicates that the battery remains charged or always remains discharged, $\min(|I(k)|, |I(k-1)|)$ is the smaller of $|I(k)|$ and $|I(k-1)|$. In order to increase the robustness of the system, an adaptive weighting factor $\lambda(k)$ is introduced, which is adjusted according to the status of the current charge and discharge and the magnitude of identification error

$$\lambda(k) = \begin{cases} 1 - \frac{e^2(k-1)}{1 + \varphi^T(k-1)P(k-1)\varphi(k-1)}, & \delta=0 \\ \lambda=1, & \delta=1 \end{cases} \quad (16)$$

where $e(k-1) = y(k-1) - \varphi^T(k-1)\hat{\theta}(k-1)$.

Extended Kalman filter (EKF) can make the optimal estimation of the target state under the minimum variance, which is often used in SOC estimation of lithium iron phosphate batteries. For the nonlinear system, the state equation of discrete space is as follows:

$$\begin{cases} x_k = f(x_{k-1}, u_{k-1}) + \omega_{k-1} \\ z_k = h(x_k) + v_k \end{cases} \quad (17)$$

where x_k represents the state of the system at time k , $x_k \in R^n$, u_k represents the control variable, z_k represents the measurement vector, $z_k \in R^n$, ω_k and v_k represent process noise and measurement noise, respectively, ω_k and v_k are uncorrelated and subject to Gaussian distribution, Q_k and R_k are covariance, $f(\cdot)$ and $h(\cdot)$ are nonlinear functions.

Firstly, the nonlinear functions $f(\cdot)$ and $h(\cdot)$ are linearized,

$$A_k = \frac{\partial f}{\partial x_k} = \begin{bmatrix} 1 & 0 & 0 \\ 0 & e^{-\frac{T}{R_1 C_1}} & 0 \\ 0 & 0 & e^{-\frac{T}{R_2 C_2}} \end{bmatrix} \quad (18)$$

$$C_k = \frac{\partial g}{\partial x_k} = \left[\frac{\partial V_T}{\partial z} \Big|_{z=z_k} \quad -1 \quad -1 \right] \quad (19)$$

The extended Kalman filter algorithm is shown in Table 2.

Table 2. Summary of the extended Kalman filter (EKF).

1 Parameter initialization: $x_0 = E(x_0)$, $P_0 = E[(x_0 - \hat{x}_0)(x_0 - \hat{x}_0)^T]$	(20)
2 State Prediction: $\hat{x}_{k+1 k}^- = f(\hat{x}_{k k}, u_k) + \omega_k$ $P_{k+1 k} = A_k P_{k k} A_k^T + Q_k$	(21)
3 Kalman filter gain: $K_{k+1} = P_{k+1 k} C_k^T [C_k P_{k+1 k} C_k^T + \hat{R}_k]^{-1}$	(22)
4 Measure values updated: $\hat{z}_{k+1} = h(\hat{x}_{k k}) + v_k$	(23)
5 Posteriori estimates: $\hat{x}_{k+1} = \hat{x}_{k+1 k}^- + K(z_{k+1} - \hat{z}_{k+1})$ $P_{k+1 k+1} = [I - K_{k+1} C_k] P_{k+1 k}$	(24)

where x_0 represents the initial state value, P_0 represents the initial covariance, $\hat{x}_{k+1|k}^-$ represents the $k+1$ prior estimate, $P_{k+1|k}$ represents the $k+1$ prior covariance, $P_{k|k}$ represents the k

prior covariance, K_{k+1} represents the Kalman gain of $k+1$, \hat{x}_{k+1} represents the $k+1$ posterior estimate, $P_{k+1|k+1}$ represents the $k+1$ covariance.

In combination with the forgetting factor adaptive least squares parameter identification and EKF algorithm, the battery SOC estimation strategy is shown in Figure 3.

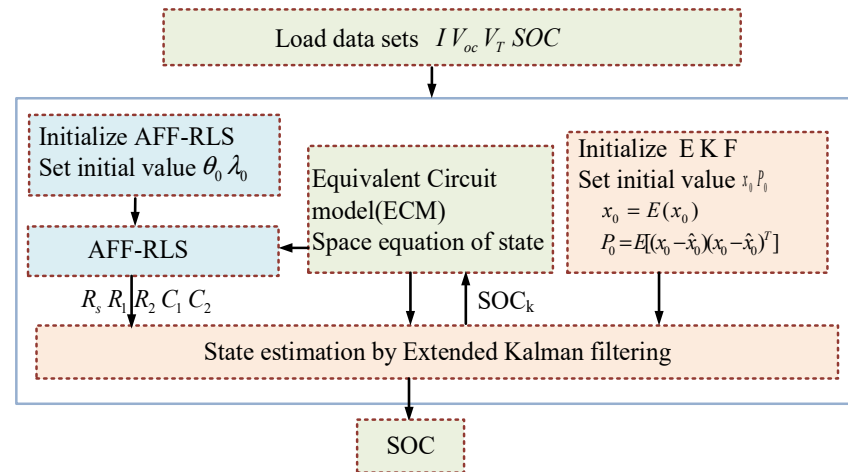


Figure 3. Adaptive forgetting factor regression least-squares—extended Kalman filter (AF-FRLS—EKF) algorithm flow chart.

4. Simulation Results and Analysis

The current curve is shown in Figure 4, and the terminal voltage curve is shown in Figure 5. The current remains positive during 0 to 166 min, which indicates the battery is in the discharge state. When $t_i = 166$ min, the state of the battery changes from the discharge state changes to the open-circuit state. When $t_i = 333$ min, the battery changes from open-circuit state to charging state. The battery state changes at $t_i = 416$ min, 500 min, 666 min, 833 min, 916 min, 1000 min, 1166 min, 1333 min, and 1416 min, respectively. The battery terminal voltage curve is shown in Figure 4, In the battery charging time interval, the measured value of the battery terminal voltage increases, while the voltage at the end of the discharge interval decreases. In the open circuit interval of the battery, the terminal voltage remains unchanged, with slight changes due to the soft changes in the terminal voltage caused by the discharge phenomenon in the R_1C_1 circuit and the R_2C_2 circuit.

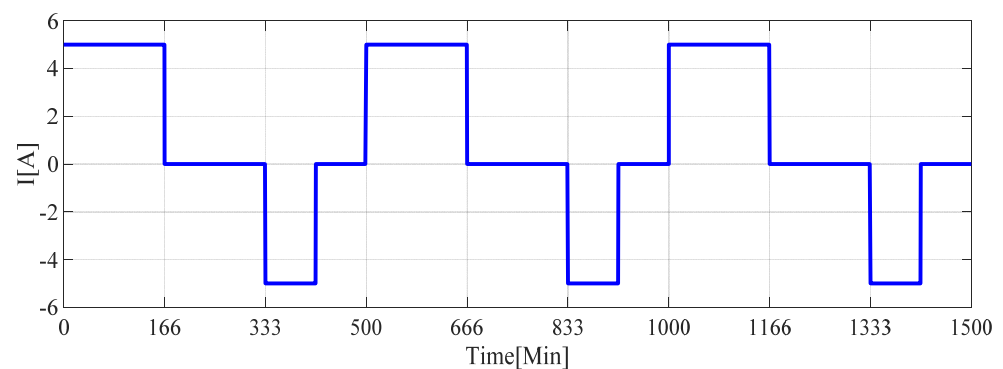


Figure 4. Current curve.

Set the initial value $\theta_0 = [0.4 \ 0.26 \ 0.22 \ -0.065 \ -2.0481]$, $P_0 = 10^3 * E_5$, where E_5 is the fifth-order identity matrix. The simulation was carried out in Matlab, and the results were shown in Figures 6 and 7. Substitute the estimated results of parameters R_s , R_l , R_2 , C_1 , and C_2 into Equation (4) to calculate the estimated terminal voltage V_T . By comparing the estimated V_T with the actual measured V_T , the estimation accuracy of terminal voltage can reflect the estimation accuracy of each parameter.

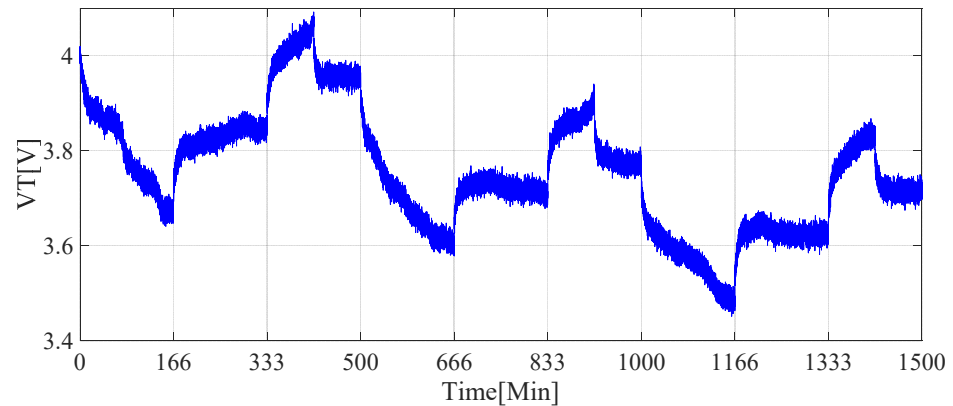


Figure 5. Terminal voltage curve.

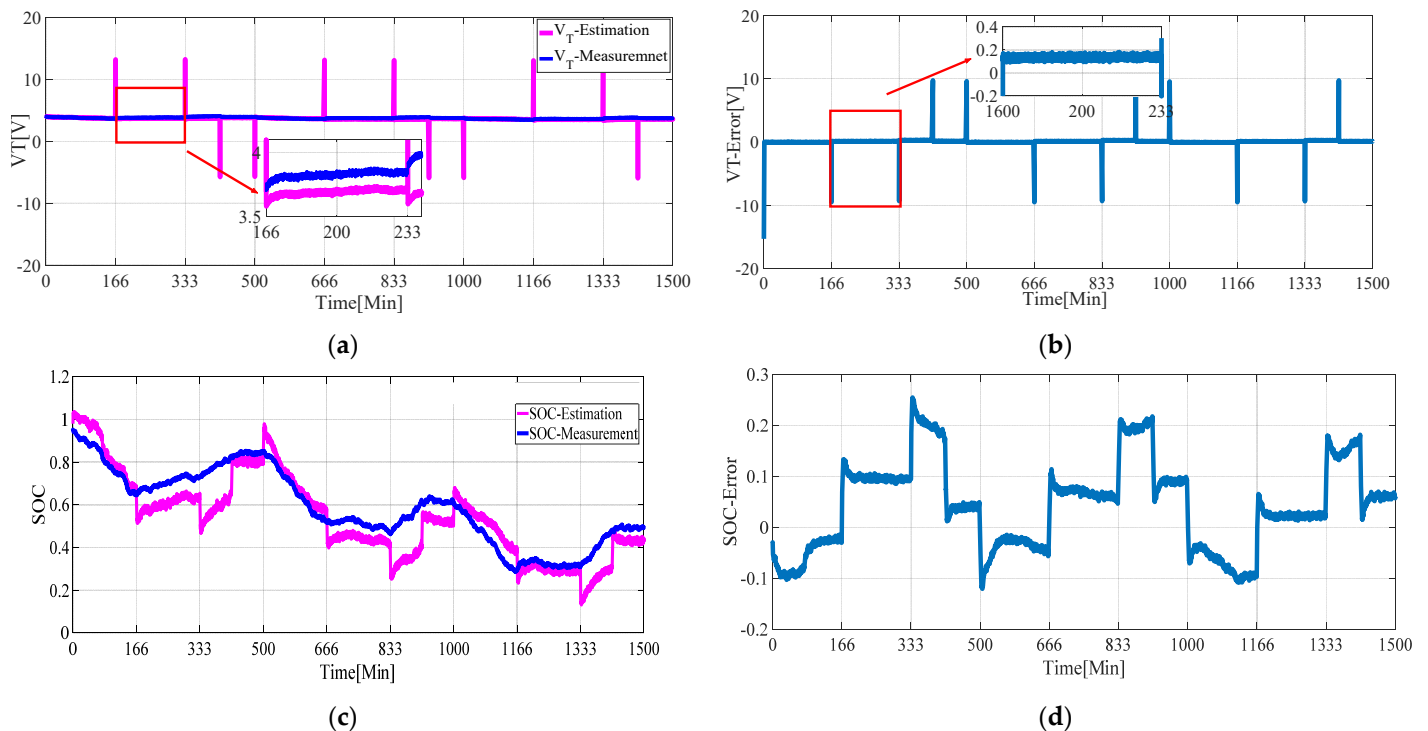


Figure 6. Regression least-squares—extended Kalman filter (RLS—EKF) algorithm. (a) Estimated terminal voltage and measured terminal voltage; (b) estimated terminal voltage error; (c) estimated state of charge (SOC) and measured SOC; (d) estimated SOC error.

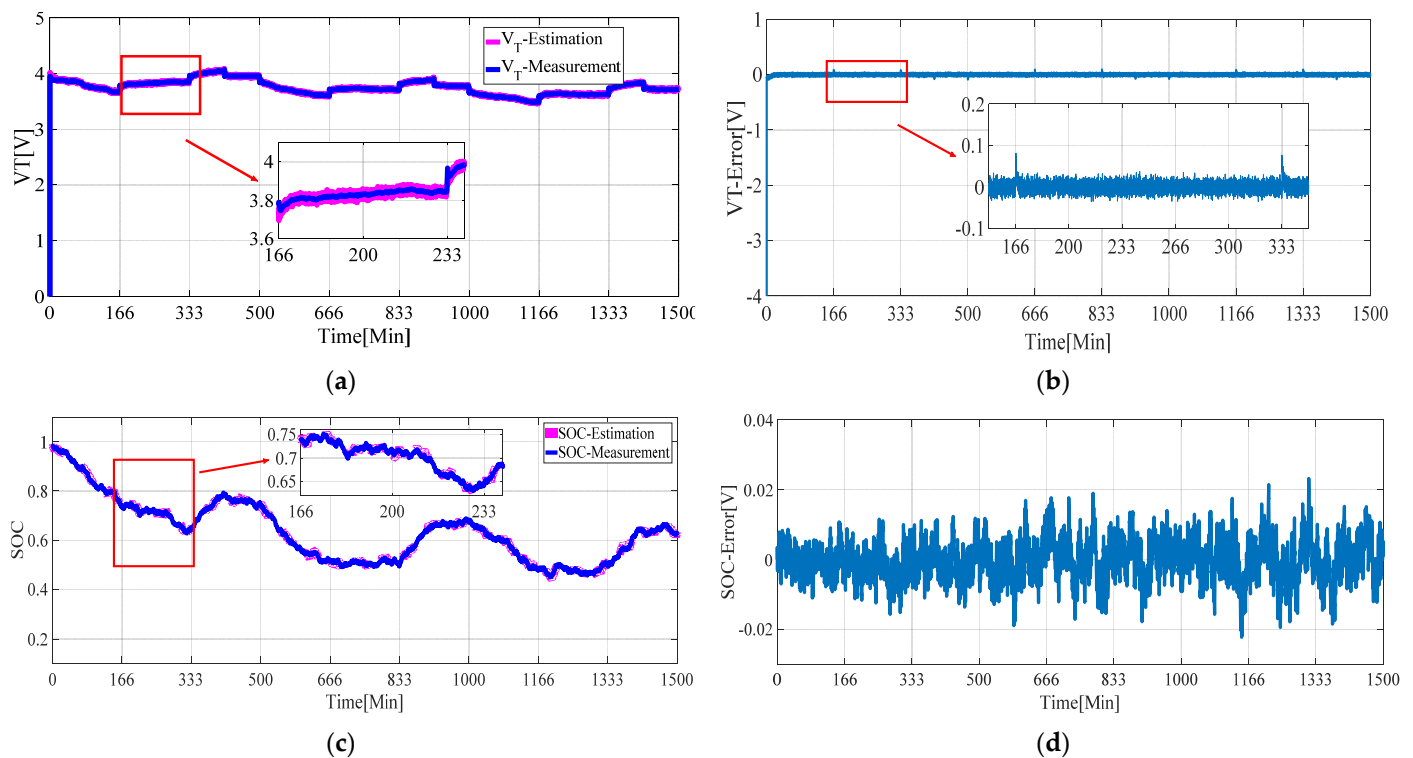


Figure 7. AFFRLS—EKF algorithm. (a) Estimated terminal voltage and measured terminal voltage; (b) estimated terminal voltage error; (c) estimated SOC and measured SOC; (d) estimated terminal voltage error.

As can be seen from Figure 6a, the error of terminal voltage is large at several time moments when the battery state changes, indicating that when the battery state changes, the estimation of parameters by the general least square algorithm fluctuates greatly, with the maximum error reaching 9.3789 V. When the battery state remains unchanged, the performance of the least square algorithm is high, and the estimation error of terminal voltage is kept within 0.2 V, as shown in Figure 6b. Based on parameter estimation, EKF is used to carry out SOC estimation. The SOC estimation results are shown in Figure 6c,d. At several special time moments when the battery state changes, the parameter estimation error is large and the SOC estimation error suddenly increases. In the time interval when the battery state remains unchanged, the parameter estimation effect is good, but the SOC estimation error is relatively weak.

The estimation results of the AFFRLS-EKF algorithm proposed in this paper are shown in Figure 7.

As can be seen from Figure 7a, the estimation result of terminal voltage is very good. Even at the moment of battery state suddenly change, the estimation error of terminal voltage is less than 0.1 V, which greatly reduces the transient error of terminal voltage estimation at the moment of battery state sudden change. As can be seen from Figure 7b, the voltage estimation error is less than 0.0439 V in the battery state retention time interval. It is shown that the proposed AFFRLS-EKF algorithm can not only improve the dynamic performance but also improve the estimation accuracy in a steady state. It can be seen from Figure 7c that the estimation effect of SOC is very good, and the estimation error is kept within 2.3%.

5. Conclusions

Aiming at the inaccurate estimation of battery parameters caused by the change of current charging and discharging state, this paper proposes a forgetting factor adaptive least-square parameter identification algorithm. Based on the accurate identification of the second-order equivalent circuit model, the battery SOC is estimated by combining

with EKF. Compared with the RLS-EKF algorithm, the algorithm proposed in this paper can better suppress the estimation error of terminal voltage when the battery state changes and improve the estimation accuracy of SOC during the steady-state.

The current flowing through series lithium-ion batteries must be strictly equal, but differences between series batteries can cause the battery to overcharge or discharge during the charge and discharge process [41,42]. This will make a significant impact on battery life, battery safety, and battery capacity utilization efficiency. In order to ensure the consistency of the voltage between the series battery cells, it is very important to balance the charge and discharge. In a BMS, a battery equalizer is used to achieve voltage consistency between series-connected battery cells. Therefore, the influence of voltage consistency between battery cells in series on the state estimation of the battery management system will be considered in the subsequent research.

Author Contributions: Conceptualization, Y.Z. (Yingjie Zhang) and J.Z.; methodology, and writing—original draft preparation, M.L.; software, Z.H.; validation, Y.Z. (Ying Zhang) funding acquisition, Y.Z. (Yingjie Zhang). All authors have read and agreed to the published version of the manuscript.

Funding: This research was jointly funded by National Key Research and Development Program of China, grant number 2019YFE0105300”, Strategic Emerging Industry Science and Technology Tackling and Major Achievements Transformation Project of Hunan Province named Key Technology of Water Supply Network Leakage Control Based on Supercomputing and Its Engineering Application, grant number 2019GK4030, and Hunan Water Metering Information Engineering Technology Research Center 2020TP2018. “The APC was funded by National Key Research and Development Program of China, grant number 2019YFE0105300”.

Institutional Review Board Statement: Not applicable.

Informed Consent Statement: Not applicable.

Data Availability Statement: Data available in a publicly accessible repository that does not issue DOIs. Publicly available datasets were analyzed in this study. This data can be found here: [https://github.com/jdorsey22/298-Estimation-Theory/blob/master/EKF/DataFiles/IV_data_nonlinear.mat]. Accessed on 1 January 2021].

Conflicts of Interest: The authors declare no conflicts of interest.

References

1. Gabbar, H.A.; Othman, A.M.; Abdussami, M.R. Review of Battery Management Systems (BMS) Development and Industrial Standards. *Technologies* **2021**, *9*, 28.
2. Hu, Y.; Wang, Y. Two Time-Scaled Battery Model Identification with Application to Battery State Estimation. *IEEE Trans. Control. Syst. Technol.* **2015**, *23*, 1180–1188, doi:10.1109/tcst.2014.2358846.
3. Zhang, Y.; Ai, Z.; Chen, J.; You, T.; Du C.; Deng, L. Energy-Saving Optimization and Control of Autonomous Electric Vehicles 261 With Considering Multiconstraints. *IEEE Trans Cybern*, 2021, 1–13.
4. Lipu, M.S.H.; Hannan, M.A.; Ayob, A.; Saad, M.H.M.; Hussain, A. Review of lithium-ion battery state of charge estimation methodologies for electric vehicle application. *Int. J. Eng. Technol.* **2018**, *7*, 219–224.
5. Zhang, Y.; Song, W.; Lin, S.; Feng, Z. A novel model of the initial state of charge estimation for LiFePO₄ batteries. *J. Power Sources* **2014**, *248*, 1028–1033, doi:10.1016/j.jpowsour.2013.09.135.
6. Kwak, M.; Lkhagvasuren, B.; Park, J.; You, J. Parameter Identification and SOC Estimation of a Battery under the Hysteresis Effect. *IEEE Trans. Ind. Electron.* **2020**, *67*, 9758–9767.
7. Farmann, A.; Waag, W.; Marongiu, A.; Sauer, D.U. Critical review of on-board capacity estimation techniques for lithium-ion batteries in electric and hybrid electric vehicles. *J. Power Sources* **2016**, *281*, 114–130.
8. Zhu, W.; Sun, Q.; Gao, H. Optimized SOC estimation method for ICDKF battery based on online parameter identification. *Chin. J. Power Resour.* **2020**, *44*, 97–102.
9. Xing, Y.; Ma, E.W.M.; Tsui, K.L.; Pecht, M. Battery Management Systems in Electric and Hybrid Vehicles. *Energies* **2011**, *4*, 1840–1857, doi:10.3390/en4111840.
10. Lelie, M.; Braun, T.; Knips, M.; Nordmann, H.; Ringbeck, F.; Zappen, H.; Sauer, D.U. Battery Management System Hardware Concepts: An Overview. *Appl. Sci.* **2018**, *8*, 534.
11. Lee, J.; Kim, J.-M.; Yi, J.; Won, C.-Y. Battery Management System Algorithm for Energy Storage Systems Considering Battery Efficiency. *Electronics* **2021**, *10*, 1859.

12. Samanta, A.; Chowdhuri, S.; Williamson, S.S. Machine Learning-Based Data-Driven Fault Detection/Diagnosis of Lithium-Ion Battery: A Critical Review. *Electronics* **2021**, *10*, 1309.
13. Aiello, O. Electromagnetic Susceptibility of Battery Management Systems' ICs for Electric Vehicles: Experimental Study. *Electronics* **2020**, *9*, 510.
14. Kang, T.; Park, S.; Lee, P.-Y.; Cho, I.-H.; Yoo, K.; Kim, J. Thermal Analysis of a Parallel-Configured Battery Pack (1S18P) Using 21700 Cells for a Battery-Powered Train. *Electronics* **2020**, *9*, 447.
15. Abbas, M.; Cho, I.; Kim, J. Analysis of High-Power Charging Limitations of a Battery in a Hybrid Railway System. *Electronics* **2020**, *9*, 212.
16. Arnieri, E.; Boccia, L.; Amoroso, F.; Amendola, G.; Cappuccino, G. Improved Efficiency Management Strategy for Battery-Based Energy Storage Systems. *Electronics* **2019**, *8*, 1459.
17. Lee, S.; Kim, J. Power Capability Analysis of Lithium Battery and Supercapacitor by Pulse Duration. *Electronics* **2019**, *8*, 1395.
18. Uno, M.; Ueno, T.; Yoshino, K. Cell Voltage Equalizer Using a Selective Voltage Multiplier with a Reduced Selection Switch Count for Series-Connected Energy Storage Cells. *Electronics* **2019**, *8*, 1303.
19. Lee, H.; Park, J.; Kim, J. Incremental Capacity Curve Peak Points-Based Regression Analysis for the State-of-Health Prediction of a Retired LiNiCoAlO₂ Series/Parallel Configured Battery Pack. *Electronics* **2019**, *8*, 1118.
20. Sun, F.; Hu, X.; Yuan, Z.; Li, S. Adaptive unscented Kalman filtering for state of charge estimation of a lithium-ion battery for electric vehicles. *Fuel. Energy. Abs.* **2014**, *5*, 3531–3540.
21. Lim, K.C.; Bastawrous, H.A.; Duong, V.H.; See, K.W.; Zhang, P.; Dou, S.X. Fading Kalman filter-based real-time state of charge estimation in LiFePO₄ battery-powered electric vehicles. *Appl. Energy* **2016**, *169*, 40–48.
22. He, H.; Xiong, R.; Zhang, X.; Sun, F.; Fan, J. State-of-Charge Estimation of the Lithium-Ion Battery Using an Adaptive Extended Kalman Filter Based on an Improved Thevenin Model. *IEEE Trans. Veh. Technol.* **2011**, *4*, 1461–1469.
23. He, Z.; Yang, Z.; Cui, X.; Li, E. A Method of State-of-Charge Estimation for EV Power Lithium-Ion Battery Using a Novel Adaptive Extended Kalman Filter. *IEEE Trans. Veh. Technol.* **2020**, *69*, 14618–14630.
24. Song, Q.; Mi, Y.; Lai, W. A Novel Variable Forgetting Factor Recursive Least Square Algorithm to Improve the Anti-Interference Ability of Battery Model Parameters Identification. *IEEE Access* **2019**, *7*, 61548–61557.
25. Xie, W.; Zhao, Y.; Fang, Z.; Liu, S. Parameter Identification Method for Equivalent Model of Supercapacitor Module with Variable Forgetting Factor Recursive Least Square Method. *Trans. Chin. Electron. Soc.* **2021**, *5*, 996–1005.
26. Rijanto, E.; Rozaqi, L.; Nugroho, A.; Kanarachos, S. RLS with optimum multiple adaptive forgetting factors for SoC and SoH estimation of Li-Ion battery. In *Proceedings of the 2017 5th International Conference on Instrumentation, Control, and Automation (ICA)*, Yogyakarta, Indonesia, 9–11 August 2017; IEEE Computer Society: Washington, DC, USA, 2017.
27. Li, Y.; Chen, J.; Lan, F. Enhanced online model identification and state of charge estimation for lithium-ion battery under noise corrupted measurements by bias compensation recursive least squares. *J. Power Sources* **2020**, *456*, 227984.
28. Wei, Z.; Zhao, J.; Ji, D.; Tseng, K.J. A multi-timescale estimator for battery state of charge and capacity dual estimation based on an online identified model. *Appl. Energy* **2017**, *204*, 1264–1274.
29. Sun, D.; Chen, X. Adaptive parameter identification method and state of charge estimation of lithium ion battery. In *Proceedings of the 2014 17rd International Conference on Electrical Machines and Systems (ICEMS)*, Hangzhou, China, 22–25 October 2014; IEEE Computer Society: Washington, DC, USA, 2014.
30. Qiu, Y.; Li, X.; Chen, W.; Duan, Z.; Yu, L. State of charge estimation of vanadium redox battery based on improved extended Kalman filter. *ISA Trans.* **2019**, *94*, 26–337.
31. Corno, M.; Bhatt, N.; Savaresi, S.M.; Verhaegen, M. Electrochemical model-based state of charge estimation for Li-ion cells. *IEEE Trans. Control Syst. Technol.* **2015**, *23*, 117–127.
32. Fan, G.; Li, X.; Canova, M. A reduced-order electrochemical model of li-ion batteries for control and estimation applications. *IEEE Trans. Veh. Technol.* **2018**, *67*, 76–91.
33. Prada, E.; Di Domenico, D.; Creff, Y.; Bernard, J.; Sauvante-Moynot, V.; Huet, F. Simplified electrochemical and thermal model of LiFePO₄-graphite Li-Ion batteries for fast charge applications. *J. Electrochem. Soc.* **2012**, *159*, A1508–A1519.
34. He, H.; Xiong, R.; Fan, J. Evaluation of lithium-ion battery equivalent circuit models for state of charge estimation by an experimental approach. *Energies* **2011**, *4*, 582–598.
35. Xiong, R.; Sun, F.; Chen, Z.; He, H. A data-driven multi-scale extended Kalman filtering based parameter and state estimation approach of lithium-ion polymer battery in electric vehicles. *Appl. Energy* **2014**, *113*, 463–476.
36. Xiong, R.; Sun, F.-C.; He, H.-W. Data-driven state-of-charge estimator for electric vehicles battery using robust extended Kalman filter. *Int. J. Automot. Technol.* **2014**, *15*, 89–96.
37. Westerhoff, U.; Kroker, T.; Kurbach, K.; Kurrat, M. Electrochemical impedance spectroscopy based estimation of the state of charge of lithium-ion batteries. *J. Energy Storage* **2016**, *8*, 244–256.
38. Available online: https://github.com/jdorsey22/298-Estimation-Theory/blob/master/EKF/DataFiles/IV_data_nonlinear.mat (accessed on 1 January 2021).
39. Yu, Q.Q.; Xiong, R.; Wang, L.Y.; Lin, C. A comparative study on open circuit voltage models for Lithium-ion batteries. *Chin. J. Mech. Eng.* **2018**, *31*, 651–658.
40. Zhang, T.; Yang, S.; Hu, J.; Gao, J.; Liu, D. State of charge estimation of lithium battery based on FFRLS-SRUKF algorithm. In *Proceedings of the 2020 IEEE 3rd International Conference on Electronics Technology (ICET)*, Chengdu, China, 8–11 May 2020; IEEE Computer Society: Washington, DC, USA, 2020.

-
41. Luo, X.; Kang, L.; Lu, C.; Linghu, J.; Lin, H.; Hu, B. An Enhanced Multicell-to-Multicell Battery Equalizer Based on Bipolar-Resonant LC Converter. *Electronics* **2021**, *10*, 293.
 42. Doridant, A.; Abouda, K.; Givelin, P.; Thibaud, B. Battery Management System Demonstrator Board design using EMC System simulation. In Proceedings of the 2019 International Symposium on Electromagnetic Compatibility—EMC EUROPE, Barcelona, Spain, 2–6 September 2019.